9-2011

Energy Transfer From Fluorescent Proteins To Metal Nanoparticles

Suraj Saraswat

Anil Desireddy

Desheng Zheng

Lijun Guo

H. Peter Lu
Bowling Green State University - Main Campus, hplu@bgsu.edu

See next page for additional authors

Author(s)
Suraj Saraswat, Anil Desireddy, Desheng Zheng, Lijun Guo, H. Peter Lu, Terry P. Bigioni, and Dragan Isailovic

THE JOURNAL OF PHYSICAL CHEMISTRY C

ARTICLE

pubs.acs.org/JPCC

Energy Transfer from Fluorescent Proteins to Metal Nanoparticles

Suraj Saraswat,[†] Anil Desireddy,[†] Desheng Zheng,[‡] Lijun Guo,[‡] H. Peter Lu,[‡] Terry P. Bigioni,[†] and Dragan Isailovic*[,†]

[†]Department of Chemistry, University of Toledo, Toledo, Ohio 43606, United States

[‡]Department of Chemistry, Bowling Green State University, Bowling Green, Ohio 43403, United States

ABSTRACT: Energy transfer plays a significant role in numerous chemical, physical, and biological processes. While the use of fluorescent proteins in Förster resonance energy transfer (FRET) studies of biomolecules is common, energy transfer between fluorescent proteins and inorganic nanoparticles has not been explored in detail. In this study, energy transfer from fluorescent phycobiliproteins to noble metal nanoparticles was analyzed. Solutions of B-phycoerythrin (B-PE) were mixed with colloidal Au and Ag nanoparticles and were characterized by steady-state and time-resolved fluorescence spectroscopy to determine the magnitude and mechanism of the energy transfer. It was found that the protein fluorescence was quenched after the addition of metal nanoparticles. Electron microscopy and absorption spectroscopy confirmed that B-PE was adsorbed onto the nanoparticles, creating a favorable geometry for quenching. Time-resolved fluorescence spectroscopy showed that B-PE fluorescence lifetimes decreased from 2.2 ns to 0.5 and 0.6 ns upon adsorption onto Au and Ag nanoparticles, respectively, corresponding to energy transfer efficiencies of >70%. Our results, which include lifetimes, efficiencies, and energy transfer distances, show that energy was transferred via the surface energy transfer (SET) mechanism, rather than FRET.

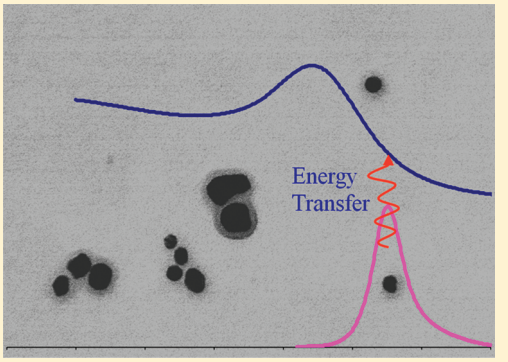

INTRODUCTION

Many useful energy transfer concepts originate from nature. For example, fluorescent proteins have evolved to perform energy transfer with extraordinary efficiency. While fluorescent proteins are commonly used as probes of protein localization in biological cells, their native functions in the host organisms are light absorption, energy transfer to other proteins, or light emission to the environment.[1] For example, green fluorescent protein (GFP) from the jellyfish *Aequorea victoria* absorbs energy transferred from blue luminescent protein (aequorin) and then emits green light.[1,2]

Cyanobacteria and eukaryotic algae (red algae, glaucophytes, and criptomonads) contain three classes of fluorescent phycobiliproteins: phycoerythrins, allophycocyanins, and phycocyanins.[3] These are assembled into photosynthetic protein complexes called phycobilisomes.[3,4] The phycobiliproteins B-phycoerythrin (B-PE) and R-phycoerythrin (R-PE) each contain more than 30 phycoerythrobilin (PEB) and phycourobilin (PUB) chromophores that are assembled in a 240 kDa multimeric complex $(\alpha\beta)_6\gamma$. Hence, phycobilin chromophores, which are linear tetrapyrole compounds bound to polypeptide chains by thioether bonds, are responsible for the excellent spectroscopic properties of phycobiliproteins as well as energy transfer involving phycobiliproteins.[4]

Phycobilisomes absorb sunlight and then transfer energy via Förster resonance energy transfer (FRET) to chlorophyll a.[4] Phycobiliproteins possess unique characteristics that make them suitable for fluorescence detection and energy transfer, which include extremely high absorption coefficients over a broad part of the visible spectrum, high fluorescence quantum yields, and large Stokes shifts.[1,5,6] For example, both B-PE and R-PE absorb light from ~450 nm to ~570 nm and emit orange fluorescence that peaks at 576 nm with quantum yields of 0.98 and 0.84, respectively.[6]

Previously, it was found that light is absorbed in phycoerythrins by phycourobilin and phycoerythrobilin chromophores.[6] Energy is then transferred to phycoerythrobilin chromophores by FRET, with subsequent emission from this chromophore at 576 nm.[7] In phycobilisomes, FRET flows from the phycobilin chromophores of phycoerythrin, located at the outer rods of the phycobilisome complex, toward the phycocyanobilin chromophores of phycocyanins and allophycocyanins.[4] The latter phycobiliproteins are located in the core of the phycobilisome complex, and energy is further transferred toward chlorophyll a. It is important to note that the energy transfer efficiency among phycobiliproteins in a phycobilisome complex is close to 100%.[4] This extremely high efficiency of energy transfer in these protein systems motivates the careful study of the energy transfer process from phycobiliproteins to technologically relevant inorganic nanomaterials, such as metal nanoparticles (NP).

Fluorescent molecules in close proximity to metal nanoparticles may exhibit changes in their spectroscopic properties. Previous studies have shown that fluorescent molecules mixed with metal nanoparticles and on metal surfaces may exhibit

Received: March 29, 2011
Revised: July 12, 2011
Published: July 14, 2011

dx.doi.org/10.1021/jp2029246 | *J. Phys. Chem. C* 2011, 115, 17587–17593

fluorescence intensities, quantum yields, and fluorescence lifetimes that are different than for the fluorophores alone.[1,8,9] Energy transfer between fluorescent molecules and nanoparticles can involve mechanisms such as surface energy transfer (SET) and electron transfer.[10−15] In addition, fluorescence intensities can decrease as a result of dynamic or static collisional quenching, thermal deactivation, charge buildup, or reactions of fluorescent molecules with impurities.[1]

Since FRET is a resonant process, it requires the emission spectrum of a donor fluorophore to overlap with the absorption spectrum of a nearby acceptor molecule. In contrast, SET does not require a resonant electronic transition, since it involves the interaction of the dipole field of the donor with the free conduction electrons of the metal.

Förster theory predicts the rate of the energy transfer, $k_T(r)$, in FRET to be the following:

$$k_T(r) = (1/\tau_D)(R_0/r)^6 \quad (1)$$

where τ_D is the lifetime of the donor in the absence of energy transfer and r is the distance between donor and acceptor molecules.[1] The Förster distance, R_0, is the distance where the nonradiative energy transfer rate equals the radiative decay rate of the donor in the absence of the acceptor.[1]

For SET, the energy transfer rate is given by the following equation:

$$k_{SET} = (1/\tau_D)(d_0/d)^4 \quad (2)$$

where d is the distance between donor and acceptor molecules and d_0 is the distance at which a fluorophore has an equal probability of nonradiative energy transfer and radiative emission, which can be calculated using Persson's and Lang's model.[10−14]

The distance dependence of FRET and SET are such that FRET tends to be operative at short distances while SET can still be effective at long distances. Experimental observations of FRET are generally limited to distances of up to ∼8 nm, whereas SET is effective for much larger distances.[10−14]

These energy transfer processes between fluorescent donor molecules and acceptors, such as metal nanoparticles, will depend on the physical and chemical characteristics of the molecules and particles involved. For example, it has been shown that the fluorescence of rhodamine 6G is quenched by gold nanoparticles of various size and shape due to energy transfer from rhodamine to the metal nanoparticles by the SET mechanism.[11,12] SET has been used to monitor conformation changes of protein bovine serum albumin adsorbed on gold nanoparticles.[13] It was also shown to be a dominant mechanism of energy transfer from fluorescent dyes that were separated from gold nanoparticles by 2−15 nm using DNA linkers.[14] In contrast, many recent studies have shown that fluorescence can increase in the presence of metal nanoparticles, via a mechanism known as metal enhanced fluorescence (MEF).[16,17] For example, it was shown recently that the fluorescence intensity of R-phycoerythrin is enhanced on the surface of silver.[18,19]

In this study, we investigate energy transfer between the fluorescent phycobiliprotein B-PE, which acts as a donor, and gold and silver nanoparticles, which act as acceptors. The different spectral characteristics of the Au and Ag nanoparticles enable the differentiation of FRET and SET, since the Au nanoparticle plasmon absorption is resonant with the B-PE emission spectrum while that for Ag is not. Lysozyme was also used in control experiments, since its native fluorescence is resonant with the plasmon absorption for Ag nanoparticles but not Au nanoparticles. Spectra of these proteins and nanoparticles are shown in Figure 1.

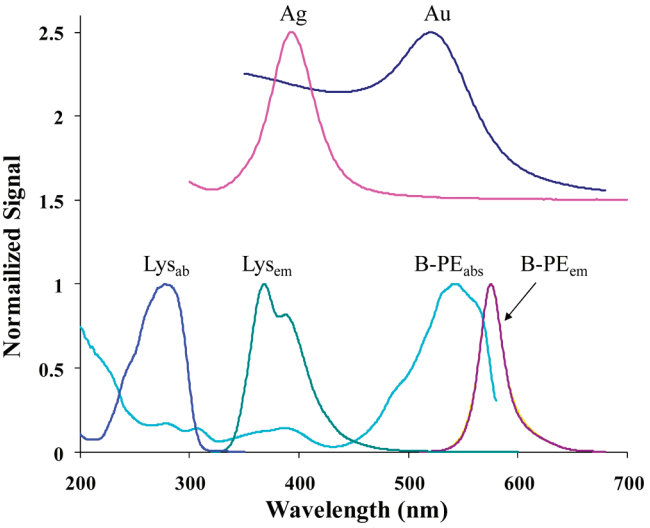

Figure 1. Absorption and emission spectra of fluorescent proteins (B-PE and lysozyme) with absorption spectra of Au and Ag colloidal nanoparticles.

Solutions of proteins were mixed with colloidal metal nanoparticles and characterized by steady-state and time-resolved fluorescence spectroscopy to elucidate the nature of the energy transfer. Electron microscopy imaging and absorption spectroscopy showed that the proteins were adsorbed to the metal nanoparticles. Time-resolved fluorescence spectroscopy measurements provided quantitative evidence for energy transfer. Excited-state lifetime measurements for the protein in the presence and in the absence of the metal nanoparticles provided a measure of energy transfer efficiency and enabled the mechanism to be identified as SET.

EXPERIMENTAL SECTION

Materials. Solutions of B-phycoerythrin (B-PE) at concentrations of 4 mg/mL were purchased from Invitrogen Molecular Probes (Eugene, OR). Lysozyme was purchased from Sigma (St. Louis, MO). Hydrogen tetrachloroaurate(III) hydrate (purity 99.999%) was purchased from Alfa Aesar (Ward Hill, MA). Sodium chloride, silver nitrate (purity 99.9%), sodium borohydride, and trisodium citrate dihydrate were purchased from Fisher Scientific (Pittsburgh, PA). HPLC grade water was purchased from Fisher for protein solutions. Purified water from a Synergy ultrapure water system from Millipore (Billerica, MA) was used for nanoparticle synthesis and substrate processing. Osmium tetroxide was purchased from Structure Probe, Inc. (West Chester, PA). 200 mesh carbon film Cu TEM grids were purchased from Electron Microscopy Sciences (Hatfield, PA).

Synthesis of Metal Nanoparticles. All reactions were carried out in water. Gold and silver nanoparticles were synthesized as described in detail elsewhere.[20,21] To synthesize gold nanoparticles, 40 ml of 1 mM hydrogen tetrachloroaurate(III) hydrate solution was heated to boiling on a hot plate. To this solution, 4 mL of 38 mM trisodium citrate solution was added all at once to the boiling solution with constant stirring (∼800 rpm). A deep red solution indicated that Au nanoparticles had formed. To synthesize silver nanoparticles, 30 mL of 2 mM sodium

borohydride and 30 drops of 38 mM trisodium citrate were first mixed together. The solution was then cooled for 15 min in an ice water bath. To this solution, 10 mL of similarly cooled 1 mM silver nitrate was added dropwise with constant stirring (~800 rpm). A bright yellow solution indicated the formation of Ag nanoparticles.

Nanoparticle Size Distributions. Scanning transmission electron microscopy (STEM) images of nanoparticles were acquired on 200 mesh copper TEM grids. Specimens were prepared for imaging by immersing the TEM grids in gold and silver nanoparticle solutions for 6 h. After that time, grids were taken out from the solution, rinsed with water, and dried with argon. Samples were imaged with a Hitachi HD-2300A 200 kV scanning transmission electron microscope (STEM). ImageJ was used to process the images and extract particle areas. Diameters were calculated assuming circular particle images, and the resulting histogram was fit with a Gaussian function. The center and half width of the Gaussian were reported as the average size and polydispersity, respectively.

Imaging of Protein Adsorption onto Nanoparticles. Samples were imaged with a JEOL JSM-7500F 30 kV SEM using a STEM detector. TEM grids were immersed in the protein−nanoparticle solution for 6 h. The grids were then rinsed with water, air-dried, and immersed in 2% osmium tetraoxide aqueous solution for 30 min. After incubation in OsO_4, the samples were rinsed with water, dried under flowing N_2, and then imaged.

Nanoparticle Absorption Spectra and Absorption Coefficients. Absorption spectra of the Ag and Au nanoparticles were measured in quartz cuvettes from 200 to 820 nm using the Nicolet Evolution 300 spectrophotometer from Thermo Electron Corporation (Madison, WI). Absorption coefficients for the nanoparticles were calculated using Beer's law, using an estimated nanoparticle concentration. The number of nanoparticles in a solution was determined from the total mass of the metal divided by the mass of spherical metal nanoparticles whose average radius was determined by STEM, as described above.

Protein Fluorescence and Fluorescence Quenching. Emission spectra of proteins in the presence and absence of metal nanoparticles were measured using the LS 50B luminescence spectrometer from PerkinElmer (Beaconsfield, Buckinghamshire, England). The emission fluorescence spectrum of B-PE was measured between 520 and 700 nm using an excitation wavelength of 490 nm and 2 mL of a 20 nM protein solution. The emission fluorescence spectrum of lysozyme was measured between 320 and 500 nm using an excitation wavelength of 280 nm and 2 mL of a 1.2 μM protein solution. Aliquots (10 μL) of Au and 20 μL aliquots of Ag nanoparticles were added to the protein solutions, and fluorescence spectra were measured. Fluorescence of protein−NP solutions was also measured after serial dilution in order to find a nanoparticle concentration range where the inner filter effect was negligible. The fluorescence intensity of the protein−nanoparticle solutions was linearly proportional to the protein concentration for the NP concentration range used, indicating that the inner filter effect was negligible. Corrected fluorescence emission spectra of phycoerythrin were measured on an Aminco Bowman II luminescence spectrometer (Thermo Scientific, Madison, WI).

Control experiments were performed to determine the effect of residual reagents from the nanoparticle synthesis on fluorescence. Residuals were added to the protein solutions by removing the NPs by precipitation and adding the supernatant. NPs were precipitated by adding 0.2 g of NaCl to a 2 mL solution of nanoparticles and then were separated from the supernatant by centrifugation at ~15 000 rpm for 5 min. Next, 1 mL of the supernatant was added to 2 mL of a 40 nM B-PE solution, and the fluorescence spectrum was measured and compared to the fluorescence spectrum of the free protein. NaCl was also added directly to the B-PE solutions to ensure that protein aggregation or precipitation did not occur.

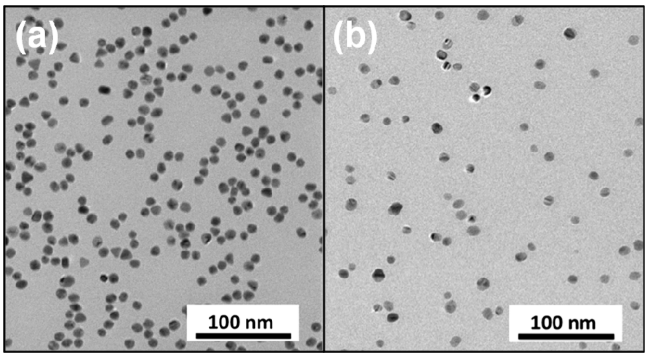

Figure 2. Scanning transmission electron microscopy images of colloidal metal nanoparticles. (a) Au nanoparticles consisted primarily of spheroids with a diameter of 10.1 ± 0.8 nm, with <5% triangular particles. (b) Ag nanoparticles were almost exclusively spheroids with a diameter of 10.3 ± 1.8 nm.

Time-Resolved Fluorescence. The detailed experimental setup for time-resolved fluorescence measurements has been described elsewhere.[22] Briefly, the fluorescence lifetimes were recorded by a time-correlated single photon counting (TCSPC) system (SPC-830, Becker & Hickl GmbH) in a single mode. The optical path for the measurement was based on the Axiovert 200M inverted scanning confocal microscope. A pulsed laser was used to excite the fluorescence with a central wavelength of 532 nm, a pulse duration of ~300 fs, and a repetition rate of 76 MHz. Both the polarization of excitation and emission were controlled by Glan Taylor polarizers. The polarized fluorescence at magic angle within 0.3 numerical aperture (NA) of the objective was collected by a single photon counting avalanche photodiode detector (MPD, module: PDM50ct). The counting rate of the signal was controlled at 500 kHz for all measurements through adjusting the intensity of the excitation laser. The lifetimes were calculated by fitting the decay curves with the convolution of a Gaussian function and exponential or biexponential decays.

RESULTS AND DISCUSSION

Properties of Nanoparticles and Fluorescent Proteins. The size and shape of the synthesized nanoparticles were determined by scanning transmission electron microscopy. It was found that gold and silver nanoparticles were predominantly spherical with diameters of 10.1 ± 0.8 nm and 10.3 ± 1.8 nm, respectively (Figure 2). The nanoparticles were further characterized by absorption spectroscopy. Plasmon absorption bands for silver and gold nanoparticles were observed at ~390 and ~525 nm, respectively (Figure 1). Steady-state fluorescence measurements show that the metal nanoparticles are not fluorescent, while B-PE has a fluorescence maximum at 576 nm. It is important to note again that the absorption spectrum of the gold nanoparticles overlaps well with the emission fluorescence spectrum of B-PE, while the absorption spectrum of Ag nanoparticles does not (Figure 1). This suggests the possibility for resonant energy transfer in the case of Au but not in the case of Ag.

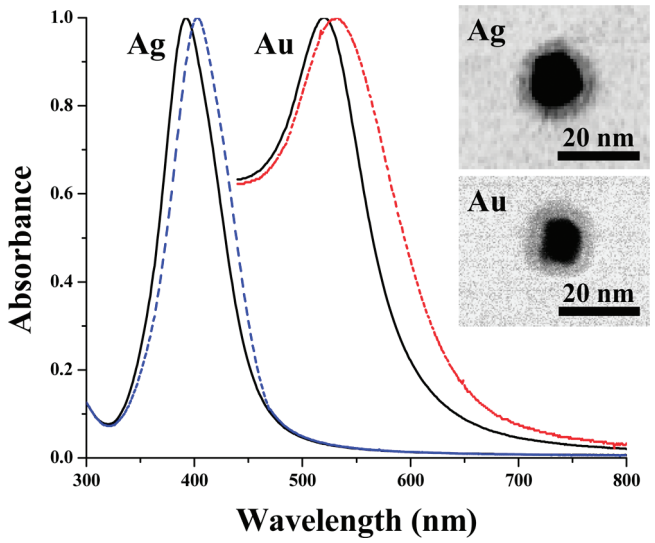

Figure 3. Absorption spectra of protein−nanoparticle suspensions (dashed curves) compared to absorption spectra of NPs (solid lines). The spectra of B-PE adsorbed on gold and silver NPs show red shifts. Insets show STEM images of B-PE adsorbed on Au and Ag NPs.

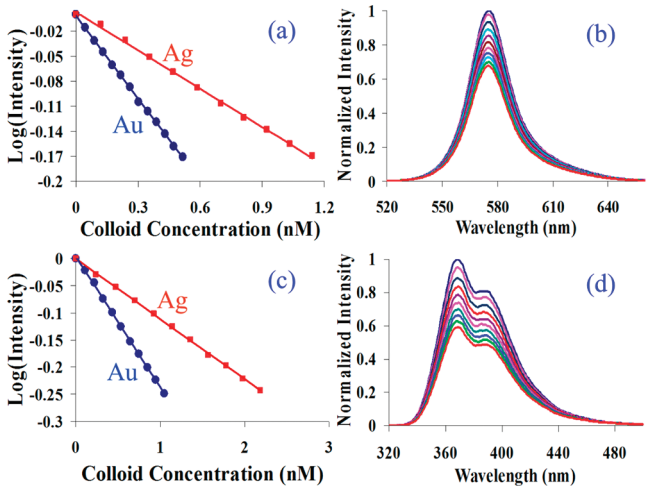

Figure 4. Semilogarithmic plots showing fluorescence intensities of (a) B-PE and (c) lysozyme as a function of Au (blue circles) and Ag (red squares) nanoparticle concentration. Fluorescence spectra of (b) B-PE with Ag nanoparticles and (d) lysozyme with Au nanoparticles.

Lysozyme's native fluorescence emission peaks at 360 nm, upon excitation at 280 nm, which is resonant with the Ag plasmon but not the Au plasmon (Figure 1). Lysozyme was therefore used as a donor, complementary to B-PE, to monitor the influence on quenching of the overlap between the emission band of the protein and the absorption band of the nanoparticles.

Adsorption of Fluorescent Proteins on Metal Nanoparticles. When nanoparticles were added to the B-PE solution, the proteins were found to adsorb onto the metal nanoparticles. The proteins were stained using osmium tetroxide, enabling their visualization under electron microscope imaging. The stained proteins were clearly visible on the surface of the nanoparticles, as shown in the insets of Figure 3. Absorption spectra also showed red shifts for the Au and Ag nanoparticle plasmons upon addition of B-PE (Figure 3), further confirming protein adsorption.[23]

Phycobiliproteins and organic fluorophores are well-known to adsorb to metal and fused silica surfaces.[8,18,19,24,25] The Au and Ag nanoparticles were protected only by citrate anions adsorbed onto their surfaces, which should not greatly impair protein adsorption. In fact, the nanoparticles appear to displace adsorbed proteins as they approach one another, leading to interparticle spacings that were much smaller than the thickness of two protein layers. Although this implies that that the proteins are physisorbed, the mechanism of adsorption is not clear. The pI of B-phycoerythrin is ∼4.4,[26] so the protein is expected to be negatively charged in pH 7 aqueous solutions. However, the particles are stabilized with citrate anions, so the adsorption of B-PE onto the metal nanoparticles is probably not electrostatic. Hydrophobic and van der Waals interactions are more likely to be involved, since these drive the self-assembly of the phycobilisome complex.[27] For lysozyme, however, the pI is 11.5,[28] so it is possible for the proteins to be electrostatically bound to the nanoparticles, although hydrophobic and van der Waals interactions could also be at play. Additionally, B-PE contains multiple cysteine residues[29] that could play a role in chemisorption, although observations of protein mobility suggest that this mechanism does not contribute to binding.

Direct imaging also facilitates estimation of the number of protein molecules adsorbed onto each individual nanoparticle. From electron microscopy, the protein layer was observed to be ∼5 nm thick. Considering that B-PE is disk shaped with a 10.1 nm diameter and 5.4 nm thickness,[30] this implies that B-PE binds to the nanoparticles oriented with its base covering the nanoparticle surface. Based on this binding geometry and the nanoparticle surface area, the number of B-PE molecules bound to NPs is estimated to be ∼4 both for gold and silver. Steady-state fluorescence was also used to estimate the number of protein molecules adsorbed onto each individual nanoparticle. By comparing the fluorescence of free protein before nanoparticle addition to the fluorescence of the supernatant after nanoparticle addition and precipitation, the number of proteins per nanoparticle was estimated to be ∼3 for Ag and ∼4 for Au.

Characterization of Phycobiliprotein−Metal Nanoparticle Mixtures by Steady-State Fluorescence Spectroscopy. Fluorescence spectra were recorded for proteins in aqueous solution mixed with aqueous colloidal metal nanoparticles. Control experiments were done to find a nanoparticle concentration range to measure fluorescence quenching with negligible influence of the inner filter effect. Steady-state fluorescence from B-PE was quenched after mixing with both Au and Ag nanoparticles (Figure 4a). Quenching was found to increase with nanoparticle concentration, but the fluorescence intensity of each mixture did not change in time. This indicated that the incubation time was shorter than the time between mixing and the first measurement, which was approximately 1 min. Similar quenching results were obtained with lysozyme in the presence of Au and Ag nanoparticles (Figure 4c). For both B-PE and lysozyme, there was no shift in the emission wavelength nor were any additional emission peaks observed (Figure 4b and d), indicating that FRET was probably not present. Control experiments showed that residual materials from the nanoparticle synthesis had no effect on the fluorescence intensities.

The steady-state fluorescence decayed exponentially with increasing nanoparticle concentration (Figure 4a and c), due to fluorescence quenching upon adsorption of the protein on the nanoparticles. It is interesting to note that fluorescence

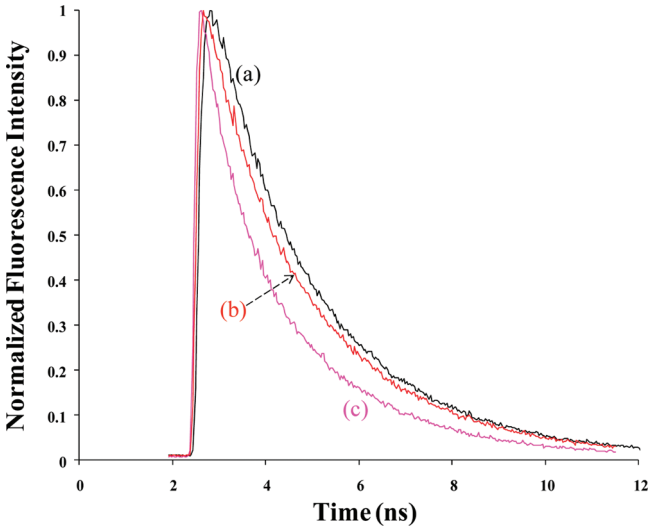

Figure 5. Time-resolved fluorescence of (a) pure B-PE, (b) B-PE incubated with Au nanoparticles, and (c) B-PE incubated with silver nanoparticles.

quenching did not depend on the overlap between the fluorescence spectrum of the protein and the absorption spectrum of the Au and Ag nanoparticles. Once adsorbed on the metal particles, the fluorophores within the proteins appeared to be stable, consistent with previous single-molecule studies.[18,19] No measurable changes in the fluorescence and absorption maxima of the proteins were observed, indicating that B-PE did not dissociate into its subunits. The native fluorescence of lysozyme was also quenched by the metal nanoparticles with no changes in the fluorescence spectrum, again indicating adsorption without disruption of the native protein fluorophores. These steady-state fluorescence results therefore indicate that neither FRET nor the dissociation of proteins were likely mechanisms of fluorescence quenching.

Energy Transfer between B-PE and Metal Nanoparticles. To determine the origin and efficiency of the energy transfer between B-PE and metal nanoparticles, excited-state lifetimes of B-PE and B-PE-nanoparticle mixtures were measured by time-resolved fluorescence spectroscopy. Measurements were performed for free B-PE and then upon addition of nanoparticles to the protein solution.

The fluorescence lifetime of B-PE was found to have decreased in the presence of gold and silver nanoparticles (Figure 5). While the intensity decay curves for pure phycobiliproteins were best fitted as monoexponential decays, the decay curves for phycobiliprotein−nanoparticle mixtures were best fitted as the sum of two exponential curves. The following biexponential decay equation was used to fit the experimental fluorescence intensity (I):

$$I(t) = y_0 + A_1 e^{-t/\tau_1} + A_2 e^{-t/\tau_2} \quad (3)$$

where t is time, τ_1 and τ_2 are decay time constants, A_1 and A_2 are the amplitudes of the two components at $t = 0$ s, and y_0 is an offset. Here, τ_1 and τ_2 correspond to fluorescence lifetimes of phycoerythrin in two different physical states: in solution and on a nanoparticle.

Monoexponential fits for pure B-PE solutions gave a lifetime of 2.24 ns, which is close to previously determined values for phycobiliproteins.[31] For the protein−nanoparticle mixtures, unconstrained biexponential fits were initially used to extract decay components that corresponded to both the free and adsorbed proteins. While the lifetimes of the first decay components closely matched that of the unbound protein, the second components were shortened. Once this was established, the τ_1 component was fixed using the free protein lifetime, and the τ_2 component for the adsorbed protein was found to be 0.5 and 0.6 ns for Au and Ag, respectively, as shown in Table 1. This was presumably due to energy transfer from the adsorbed protein to the metal nanoparticle. Note that because A_1/A_2 was higher in the Au solution than the Ag solution, its decay curve appears to be slower than that of Ag despite the decay constant for Au-bound protein being shorter.

Table 1. Time-Resolved Fluorescence Lifetimes and Energy Transfer Efficiencies of Free B-PE and B-PE Adsorbed on Metal−Nanoparticle Surfaces

system	τ_1 (ns)[a]	τ_2 (ns)[b]	ET efficiency (%)
free BPE	2.24 ± 0.01		
BPE Au	2.24 ± 0.01	0.52 ± 0.07	76.8
BPE Ag	2.24 ± 0.01	0.64 ± 0.01	71.4

[a] Lifetime of free protein. [b] Lifetime of adsorbed protein.

The energy transfer efficiency (φ_{ET}), which is the fraction of photons absorbed by the donor that are transferred to acceptor, can be determined from the fluorescence lifetimes according to the following equation:

$$\varphi_{ET} = 1 - \tau_2/\tau_1 \quad (4)$$

As shown in Table 1, energy transfer efficiencies of >70% were calculated for the mixtures of B-PE with Au and Ag nanoparticles. The similar energy transfer efficiencies for Au and Ag are contrary to what might be expected for FRET, since Ag is far from resonant with the B-PE emission band while Au is not. If FRET were operative in this case, a significant difference in the energy transfer efficiencies for the two metals would be expected. This again argues against FRET being the energy transfer mechanism.

Distances between Fluorescent Proteins and Nanoparticles. The efficiency of energy transfer is distance dependent, so it is important to calculate the distances between the fluorescent protein donors and nanoparticle acceptors. These distances can further indicate if energy is transferred through FRET or SET.

In the case of FRET, the Förster distance (R_0, in Å) can be calculated using the following equation:

$$R_0 = 0.211[\kappa^2 n^{-4} Q_{protein} J(\lambda)]^{1/6} \quad (5)$$

where κ^2 is the orientation factor (2/3 in solution), n is the refractive index of the medium (1.4), $Q_{protein}$ is the quantum yield of the protein, and $J(\lambda)$ is the overlap integral between the emission peak of the protein donor and absorption peak of the nanoparticle acceptor.[1] The overlap integral is calculated using the following equation:

$$J(\lambda) = \int F_{protein}(\lambda)\varepsilon_A(\lambda)\lambda^4 d\lambda \quad (6)$$

In this equation, $F_{protein}(\lambda)$ is the corrected fluorescence intensity of the protein, $\varepsilon_A(\lambda)$ is the absorption coefficient of the nanoparticle acceptor, and λ is the wavelength in nanometers.[1]

Table 2. Calculated Energy Transfer Parameters of Phycobiliprotein−Nanoparticle Mixtures

system	λ_{em} (nm)	$J(\lambda)$ ($M^{-1}cm^{-1}$ nm^4)	Q	R_0 (nm)	r (nm)	d_0 (nm)	d (nm)
BPE	576		0.98				
BPE Au	576	1.49×10^{18}	0.98	16.8	13.8	8.6	6.4
BPE Ag	576	1.72×10^{17}	0.98	11.7	10.0	8.6	6.9

To evaluate the overlap integral, the corrected fluorescence spectrum of the phycobiliprotein was measured, and the molar absorptivities of the nanoparticles between 520 and 700 nm were determined. Based on this analysis, the Förster distances (R_0) calculated for B-PE in the presence of gold and silver nanoparticles were 16.8 and 11.7 nm, respectively. Although these distances are large, they are consistent with previous studies[12,13] once differences in $\varepsilon_A(\lambda)$ are accounted for. In particular, the nanoparticles used in the present study are significantly larger and therefore have larger $\varepsilon_A(\lambda)$, which scales with the number of atoms in the nanoparticle.[32]

The distances (r) between fluorescent protein donors and nanoparticle acceptors were further calculated from experimentally determined values of energy transfer efficiencies, using the following equation:

$$\varphi_{FRET} = 1/(1 + (r/R_0)^6) \quad (7)$$

This analysis yielded distances between protein and metal nanoparticles of ≥10 nm (see Table 2).

To check if SET is the mechanism of energy transfer, energy transfer distances can be calculated. First, d_0 was calculated using the following equation:

$$d_0 = (0.225c^3 Q_{protein}/\omega^2_{protein}\omega_F \kappa_F)^{1/4} \quad (8)$$

where c is the speed of light (3×10^{10} cm s^{-1}), $\omega_{protein}$ is the angular frequency of the donor's electronic transition (3.27×10^{15} s^{-1}), ω_F is the angular Fermi frequency (8.4×10^{15} s^{-1} for gold and 8.3×10^{15} s^{-1} for silver), and κ_F is the Fermi wavevector (1.2×10^8 cm^{-1} for both gold and silver).[12,33] From this analysis, the calculated value of d_0 between B-PE and metal nanoparticles was 8.6 nm (Table 2).

Next, the distances (d) between donor and acceptor were calculated from the experimental energy transfer efficiencies, using the following equation:

$$\varphi_{SET} = 1/(1 + (d/d_0)^4) \quad (9)$$

Distances of 6.4 and 6.9 nm were obtained from this analysis for Au and Ag, respectively (Table 2), which are consistent with the physical dimensions of the protein−nanoparticle complex. For example, B-phycoerythrin is a disk-shaped protein with a diameter of 10.1 nm and a height of 5.4 nm,[30] while the nanoparticles have diameters of 10.2 nm. If the distance between donor and acceptor were considered to be the distance between the center of the spherical particle and center of B-PE, then the donor−acceptor pair distance would be ~7.8 nm. This estimate of the pair distance is consistent with the above calculation of SET distances.

Although the agreement is satisfactory, the slightly longer distance estimate for Ag could be due to the slightly larger average particle size and the broader size distribution. Interestingly, these distances are not consistent with the stacking of B-PE on the nanoparticles, which may be due to the disruption of the stacking geometry upon adsorption onto the nanoparticles.

The same analysis of the geometry using the FRET distance estimates are unphysical. In particular, the distance estimate for Au of 13.8 nm would put the fluorophore beyond the physical size of the protein. Further, the physical position of the fluorophore should be approximately the same with respect to the center of the nanoparticle for both Ag and Au, since the adsorption geometry should be independent of the identity of the metal. Therefore, very similar FRET distances would be expected for each metal. Estimates of the FRET distances for Au and Ag differed significantly, however, again indicating that FRET is not the operative energy transfer mechanism.

While >70% of the energy was transferred to the nanoparticles, it is interesting to account for the remaining energy. A significant fraction of the remaining energy was emitted as light, which was observed in steady-state and time-resolved fluorescence measurements. However, quantification is difficult as it was neither possible to separate the free and bound proteins nor to evaluate the quantum yield of the bound proteins. Other possibilities include an intersystem crossing to a triplet state, which could lead to radiative decay on a time scale beyond that of our measurements or nonradiative mechanisms such as internal conversion and intermolecular exciton−exciton annihilation. Whatever the fate of the remaining energy, it should be still possible to increase the energy transfer efficiency toward 100% by engineering the protein−nanoparticle couple.

CONCLUSION

When B-PE was mixed with Au and Ag nanoparticles, the proteins were found to adsorb to the metal particles, which led to fluorescence quenching. Scanning electron microscopy and absorption spectroscopy confirmed that B-PE was adsorbed on the metal nanoparticles. Time-resolved fluorescence spectroscopy showed that the energy transfer from B-PE to the metal nanoparticles occurred with >70% efficiency. The fact that energy transfer efficiencies were very similar for Au and Ag strongly suggests that FRET was not operative, since the resonance conditions were very different. Further, the SET distances between protein donors and nanoparticle acceptors were estimated to be 6.4 and 6.9 nm for Au and Ag, respectively. These distances were in agreement with estimates based on the physical size of the constituents. Estimates of FRET distances were not physically reasonable, however. These results indicate that energy was transferred from protein to nanoparticle through surface energy transfer (SET), rather than FRET. This implies that efficient energy transfer between proteins and metal nanoparticles may be possible regardless of whether or not resonance conditions are satisfied.

AUTHOR INFORMATION

Corresponding Author

*Phone: 419-530-5532; E-mail: Dragan.Isailovic@utoledo.edu.

ACKNOWLEDGMENT

This project was supported by the University of Toledo (D.I.) and NSF award numbers CBET-0955148 (T.B.) and CRIF-0840474. H.P.L. acknowledges the support from the Office of Basic Energy Sciences within the Office of Science of the U.S.

Department of Energy and from the Army Research Office of the U.S. Department of Defense.

REFERENCES

(1) Lakowicz, J. R. *Principles of Fluorescence Spectroscopy*; Springer: New York, 2006.
(2) Tsien, R. Y. *Annu. Rev. Biochem.* **1998**, *67*, 509–544.
(3) Apt, K. E.; Collier, J. L.; Grossman, A. R. *J. Mol. Biol.* **1995**, *248*, 79–96.
(4) Glazer, A. N. *Biochim. Biophys. Acta* **1984**, *768*, 29–51.
(5) Glazer, A. N.; Stryer, L. *Biophys. J.* **1983**, *43*, 383–386.
(6) Glazer, A. N.; Stryer, L. *Trends Biochem. Sci.* **1984**, *9*, 423–427.
(7) Gaigalas, A.; Gallagher, T.; Cole, K. D.; Singh, T.; Wang, L.; Zhang, Y. *Photochem. Photobiol.* **2006**, *82*, 635–644.
(8) Kemnitz, K.; Tamai, N.; Yamazaki, I.; Nakashima, N.; Yoshihara, K. *J. Phys. Chem.* **1986**, *90*, 5094–5101.
(9) Avouris, P.; Persson, B. N. J. *J. Phys. Chem.* **1984**, *88*, 837–848.
(10) Persson, B. N. J.; Lang, N. D. *Phys. Rev. B* **1982**, *26*, 5409–5415.
(11) Sen, T.; Sadhu, S.; Patra, A. *Appl. Phys. Lett.* **2007**, *91*, 043104.
(12) Sen, T.; Patra, A. *J. Phys. Chem. C* **2008**, *112*, 3216–3222.
(13) Sen, T.; Haldar, K. K.; Patra, A. *J. Phys. Chem. C* **2008**, *112*, 17945–17951.
(14) Jennings, T. L.; Singh, M. P.; Strouse, G. F. *J. Am. Chem. Soc.* **2006**, *128*, 5462–5467.
(15) Ghosh, S. K.; Pal, A.; Kundu, S.; Nath, S.; Pal, T. *Chem. Phys. Lett.* **2004**, *395*, 366–372.
(16) Lakowicz, J. R.; Ray, K.; Chowdhury, M.; Szmacinski, H.; Fu, Y.; Zhang, J.; Nowaczyk, K. *Analyst* **2008**, *133*, 1308–1346.
(17) Touahir, L.; Galopin, E.; Boukherroub, R.; Gouget-Laemmel, A. C.; Chazalviel, J. N.; Ozanam, F.; Szunerits, S. *Biosens. Bioelectron.* **2010**, *25*, 2579–2585.
(18) Ray, K.; Chowdhury, M. H.; Lakowicz, J. R. *Anal. Chem.* **2008**, *80*, 6942–6948.
(19) Chowdhury, M. H.; Ray, K.; Aslan, K.; Lakowicz, J. R.; Geddes, C. D. *J. Phys. Chem. C* **2007**, *111*, 18856–18863.
(20) Turkevich, J.; Stevenson, P. C.; Hillier, J. *Discuss. Faraday Soc.* **1951**, *11*, 55–75.
(21) Creighton, J. A.; Blatchford, C. G.; Albrecht, M. G. *J. Chem. Soc. Faraday Trans. 2* **1979**, *75*, 790–798.
(22) Guo, L.; Wang, L.; Lu, H. P. *J. Am. Chem. Soc.* **2010**, *132*, 1999–2004.
(23) Haes, A. J.; Van Duyne, R. P. *Anal. Bioanal. Chem.* **2004**, *379*, 920–930.
(24) Thobhani, S.; Attree, S.; Boyd, R.; Kumarswami, N.; Noble, J.; Szymanski, M.; Porter, R. A. *J. Immunol. Methods* **2010**, *356*, 60–69.
(25) Kang, S. H.; Yeung, E. S. *Anal. Chem.* **2002**, *74*, 6334–6339.
(26) Glazer, A. N.; Hixson, C. S. *J. Biol. Chem.* **1977**, *252*, 32–42.
(27) Zilinskas, B. A.; Glick, R. E. *Plant Physiol.* **1981**, *68*, 447–452.
(28) Wetter, L. R.; Deutsch, H. F. *J. Biol. Chem.* **1951**, *192*, 237–242.
(29) Sidler, W.; Kumpf, B.; Suter, F.; Klotz, A. V.; Glazer, A. N.; Zuber, H. *Biol. Chem. Hoppe-Seyler* **1989**, *370*, 115–124.
(30) Gantt, E. *Plant Physiol.* **1969**, *44*, 1629–1638.
(31) Guard-Friar, D.; MacColl, R.; Berns, D. S.; Wittmershaus, B.; Knox, R. S. *Biophys. J.* **1985**, *47*, 787–793.
(32) Link, S.; Wang, Z. L.; El-Sayed, M. A. *J. Phys. Chem. B* **1999**, *103*, 3529–3533.
(33) Papaconstantopoulos, D. A. *Handbook of the Band Structure of Elemental Solids*; Plenum Press: New York, 1986.